Automatic Segmentation of the Right Ventricular Outflow Tract from Human MRI Data

Chloe Snyder, Robert Gorman, Yu-Ho Hsieh

Introduction: Tetralogy of Fallot (ToF)

- Most common form of congenital heart disease
- Four defects: ventricular septal defect (VSD), pulmonary stenosis, right ventricular (RV) hypertrophy, and overriding aorta
- Surgery required for VSD closure and transannular patch application

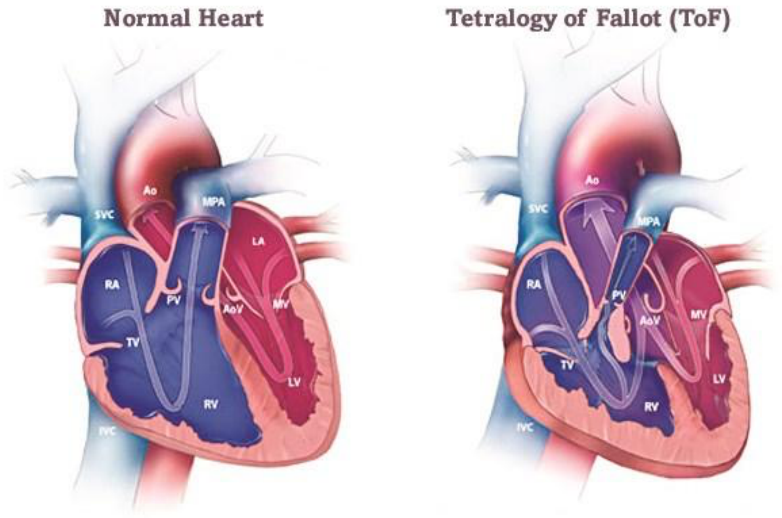

Introduction: ToF Treatment Methods

- After initial repair patients are left with pulmonary insufficiency, which leads to RV dysfunction as well as RVOT dilatation and distortion
  - Pulmonary valve replacement is often required due to these complications
- Recently, minimally invasive catheter-based approach has been developed
  - Requires detailed understanding of complex RVOT anatomy specific to the patient

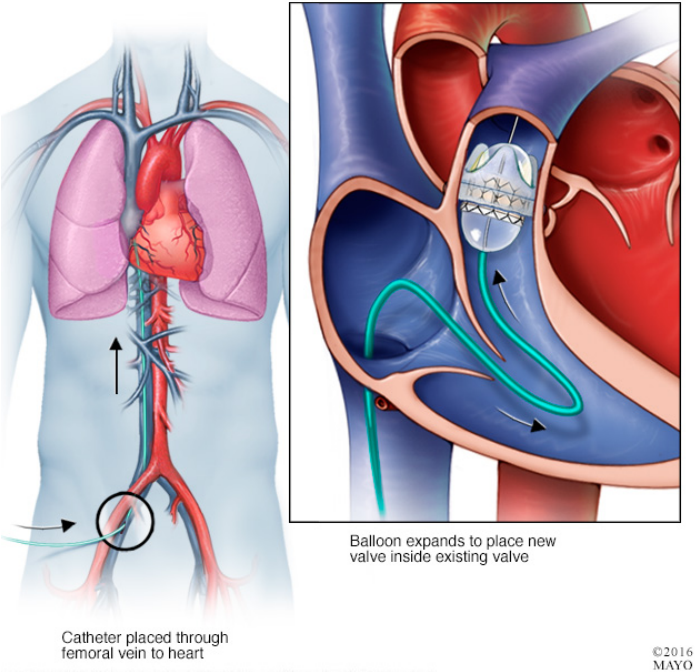

Introduction: Need for Image Analysis

- Currently, a combination of CT scanning and echocardiography are used
    - Often difficult to interpret these images without extensive experience
- We aimed to develop and validate a tool to automatically segment the RVOT in MRI data from ToF patients
    - To help facilitate 3-D quantification of individual patient anatomy

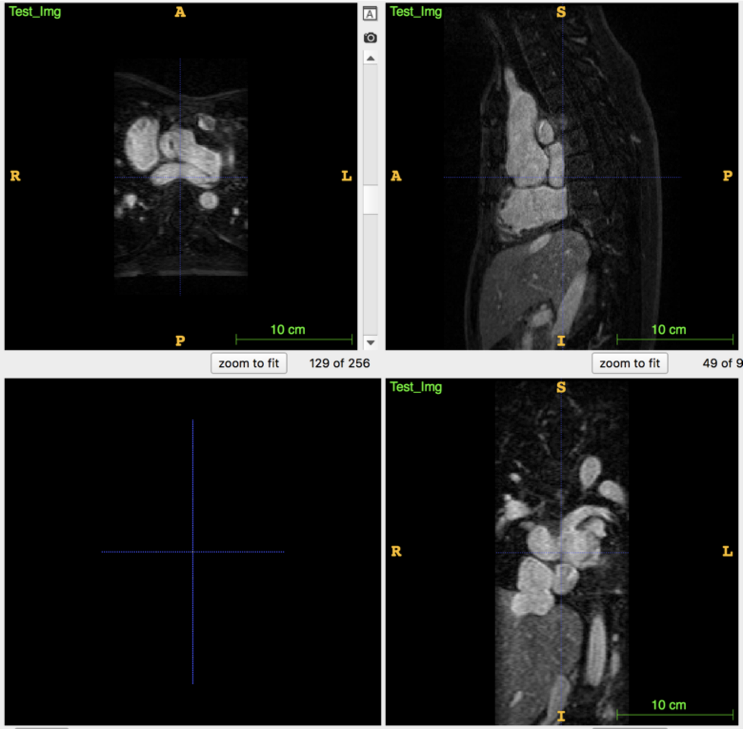

Methods: Segmentation Techniques

- 3D Active Contour approach (Snake Technique)
    - Needs images with good contrast
    - Found that our data did not have adequate contrast
- Frangi's Vesselness algorithm
    - Highlights tubular objects in an image
    - Takes a range of diameters as an input for segmentation shape prior
    - Shape prior was too general and gave undesirable results
- Multi-Atlas Segmentation technique
    - Found to be the most useful method

3D Active Contour

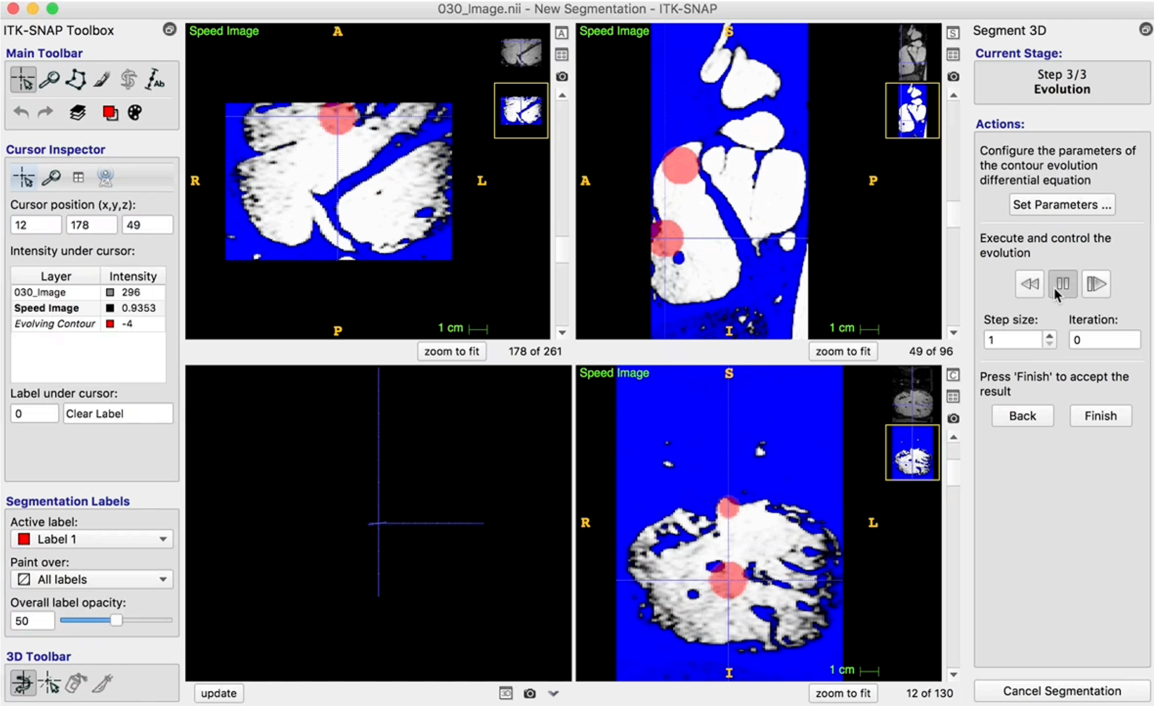

Using ITK-SNAP's snakes feature. Speed map generated by setting thresholds, which poorly segments vessels in a low contrast image

Methods: Segmentation Techniques

- 3D Active Contour approach (Snake Technique)
  - Needs images with good contrast
  - Found that our data did not have adequate contrast
- Frangi's Vesselness algorithm
  - Highlights tubular objects in an image
  - Takes a range of diameters as an input for segmentation shape prior
  - Shape prior was too general and gave undesirable results
- Multi-Atlas Segmentation technique
  - Found to be the most useful method

Frangi’s Vesselness Shape Prior

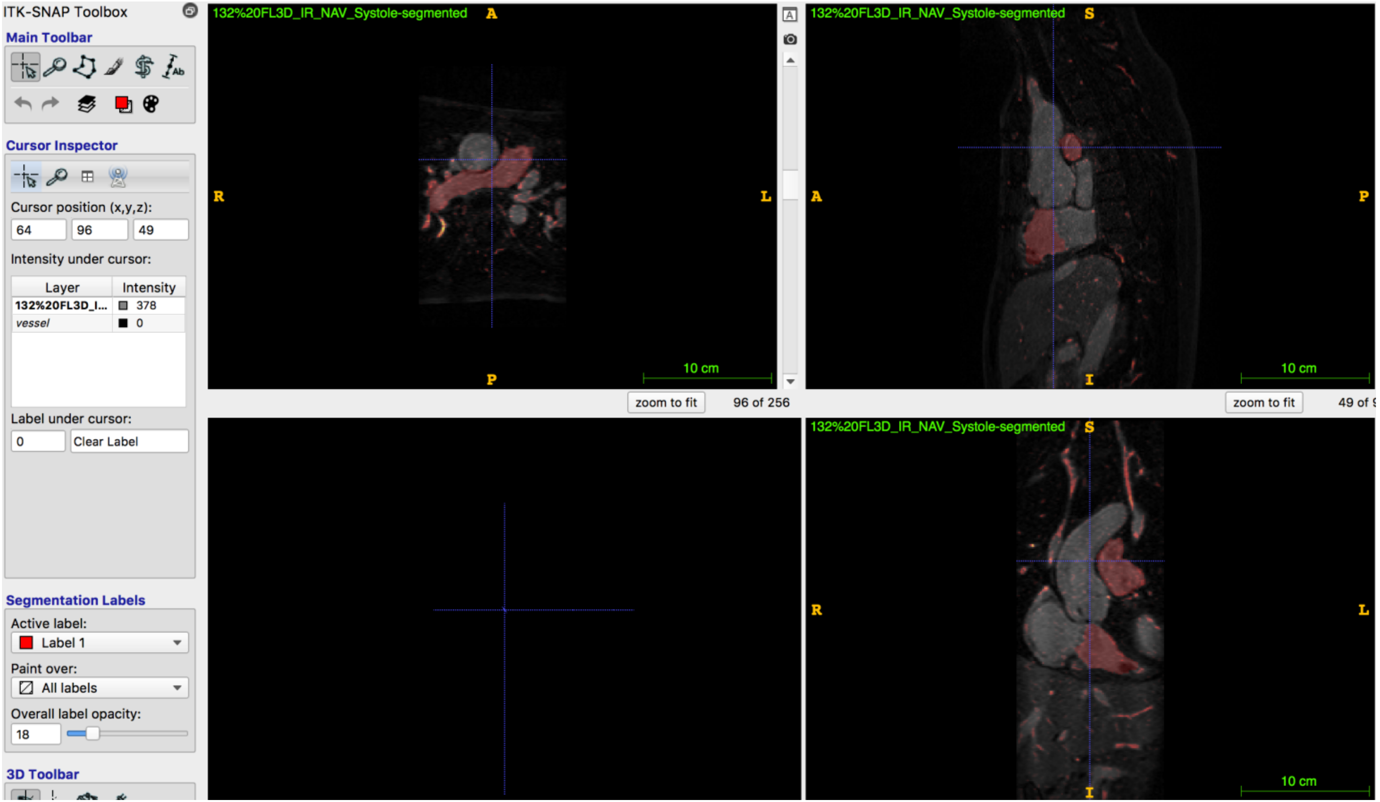

ITK-SNAP, segmentation produced by running c3d -hessobj. Parameters: Dimension: 1, Min: 1mm, Max: 1mm

Frangi’s Vesselness Shape Prior

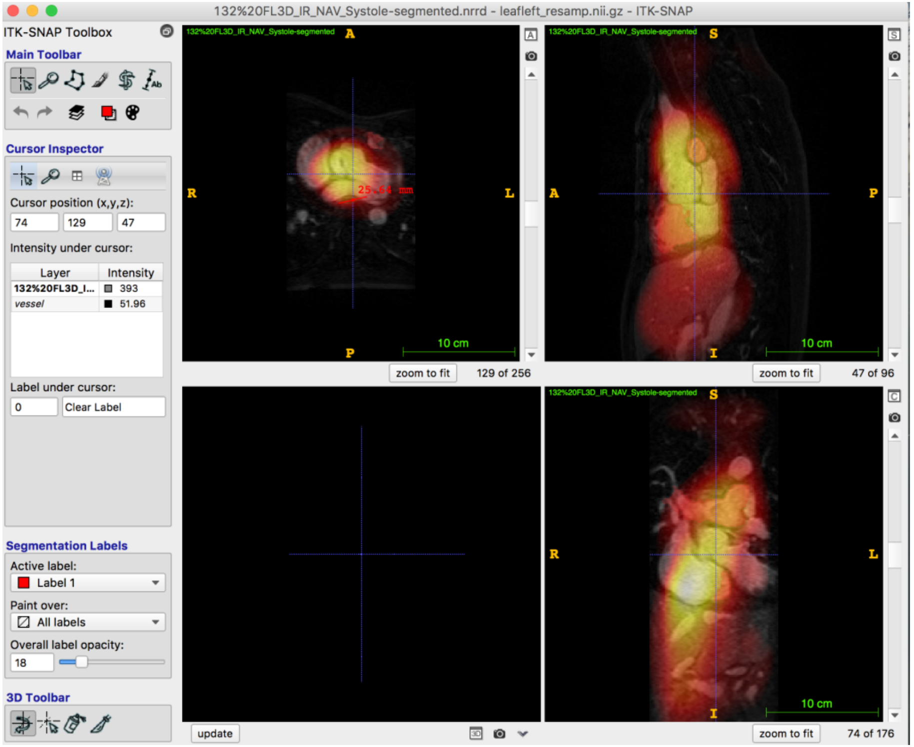

ITK-Snap, segmentation produced by running c3d -hessobj. Parameters: Dimension: 1, Min: 23mm, Max: 30mm

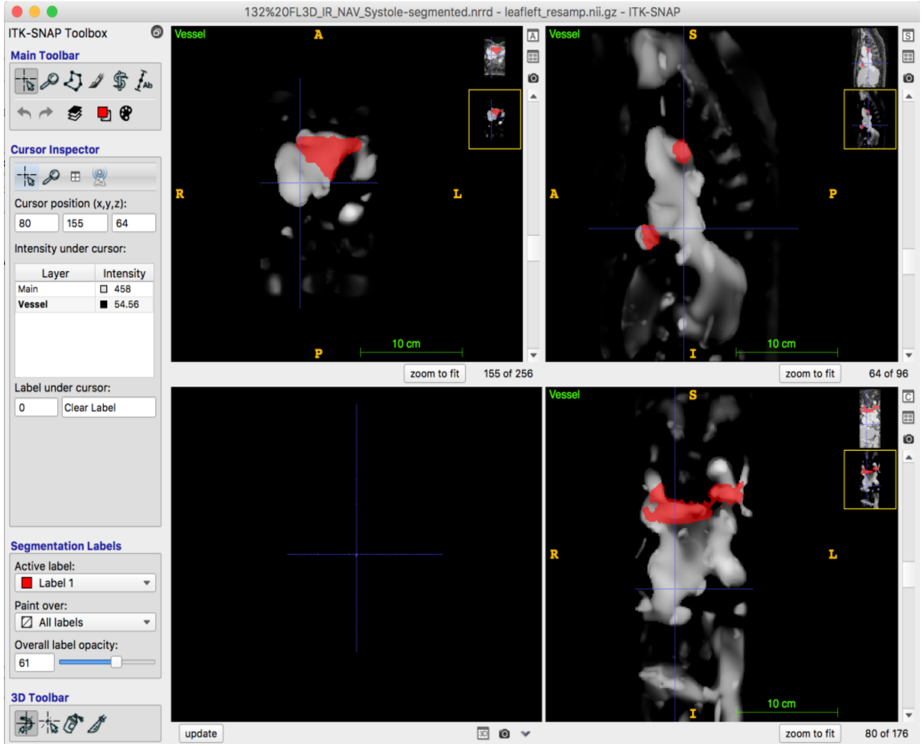

ITK-Snap, segmentation produced by running c3d -hessobj. Parameters: Dimension: 1, Min: 4mm, Max: 13mm

Methods: Multi-Atlas Segmentation

- **Treated expert manual segmentations as ground truth atlases**
- For each patient MRI, left out patient's atlas as a test image, and registered all other atlases to that patient MRI
- Each warped atlas generated a candidate segmentation of the patients MRI
- Results from each of the atlases were combined to produce the final segmentation

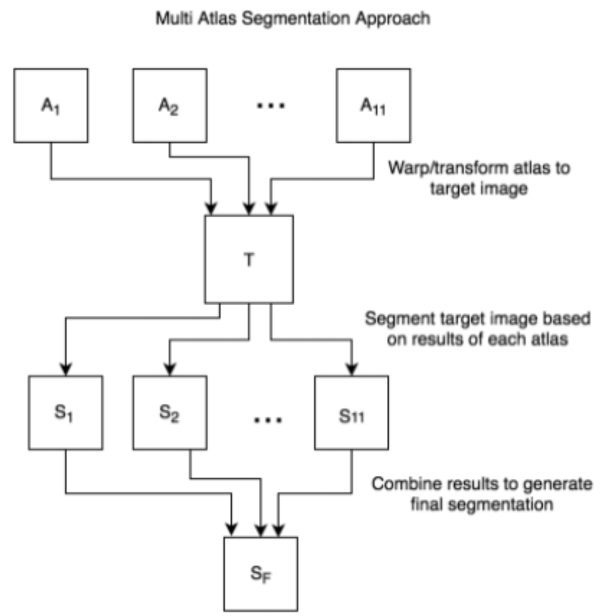

Methods: Multi-Atlas Segmentation

- Treated expert manual segmentations as ground truth atlases
- **For each patient MRI, left out patient's atlas a a test image, and registered all other atlases tc that patient MRI**
- Each warped atlas generated a candidate segmentation of the patients MRI
- Results from each of the atlases were combined t produce the final segmentation

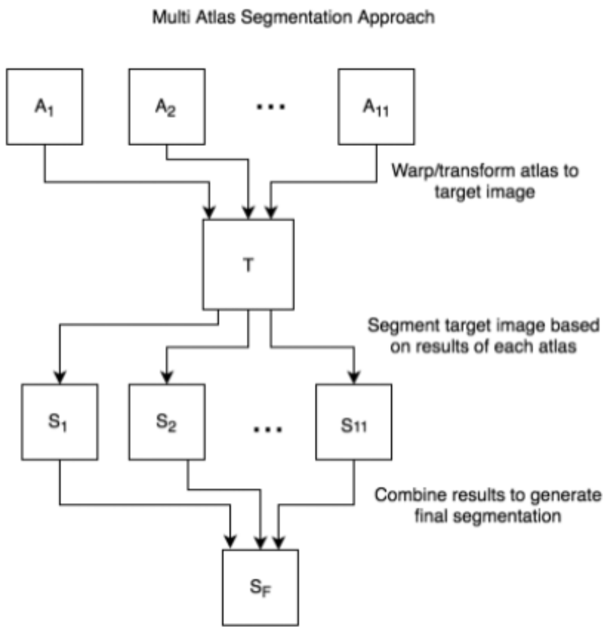

Methods: Multi-Atlas Segmentation

- Treated expert manual segmentations as ground truth atlases
- For each patient MRI, left out patient's atlas as a test image, and registered all other atlases to that patient MRI
- **Each warped atlas generated a candidate segmentation of the patients MRI**
- Results from each of the atlases were combined to produce the final segmentation

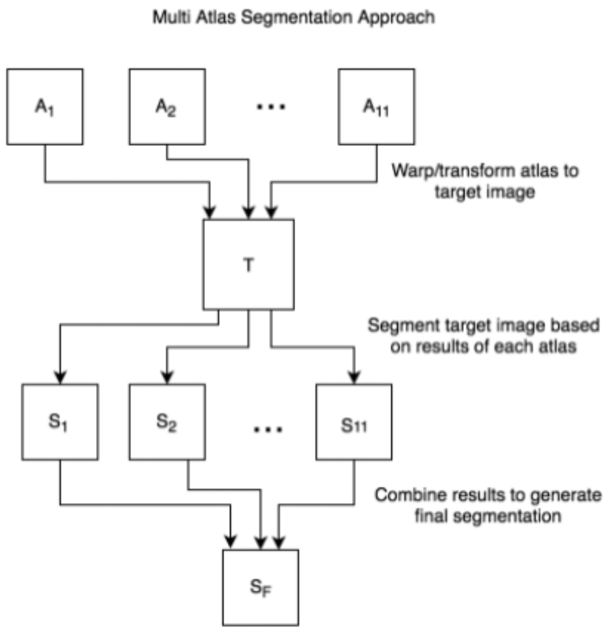

Methods: Multi-Atlas Segmentation

- Treated expert manual segmentations as ground truth atlases
- For each patient MRI, left out patient's atlas as a test image, and registered all other atlases to that patient MRI
- Each warped atlas generated a candidate segmentation of the patients MRI
- **Results from each of the atlases were combine to produce the final segmentation**

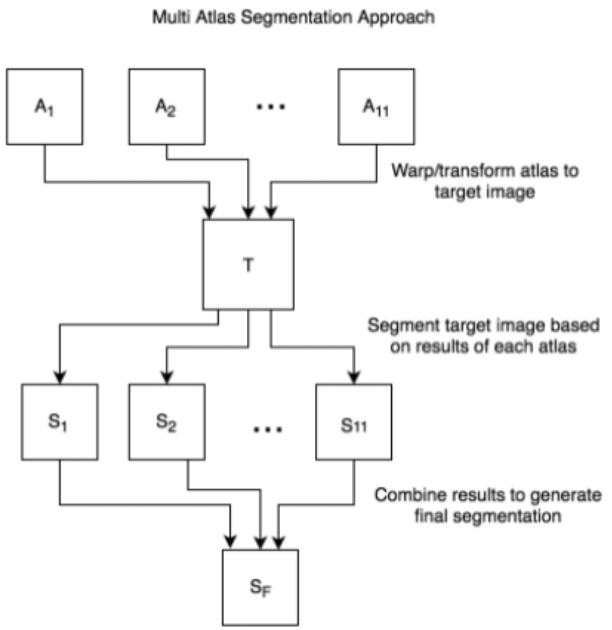

Methods: Multi-Atlas Segmentation

- **Cardiac MRIs are often difficult to register between people due to the variability of anatomy**
  - **Anatomical landmarks placed to solve this issue**
- After landmarking a homography matrix was used to map points from atlas image to corresponding points from unknown image
- Next step was deformable registration to further align images
- Followed by majority vote method to complete the segmentation
  - Determined for each voxel in each atlas whether or not the voxel is RVOT
  - If most say it is RVOT, it is labeled as such in the final segmentation

Landmarks

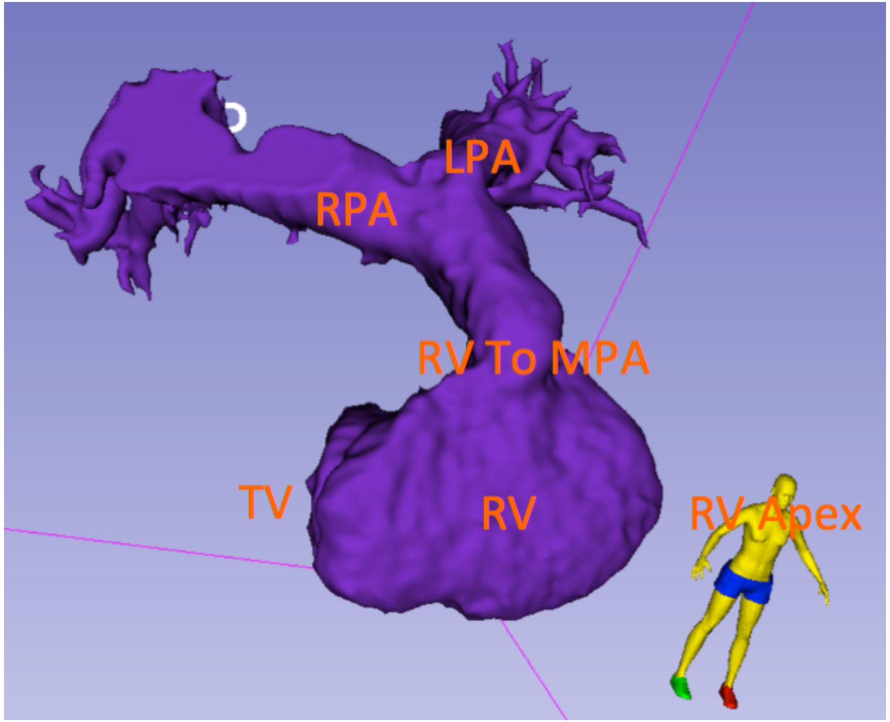

Anatomical landmarks we chose to segment the RVOT. LPA = Left pulmonary artery, RPA = right pulmonary artery, RV to MPA = right ventricle to main pulmonary artery transition, TV = tricuspid valve, RV = right ventricle. We also labeled the branching point between the MPA, LPA and RPA. Diagram courtesy of Dr. Matthew Jolley.

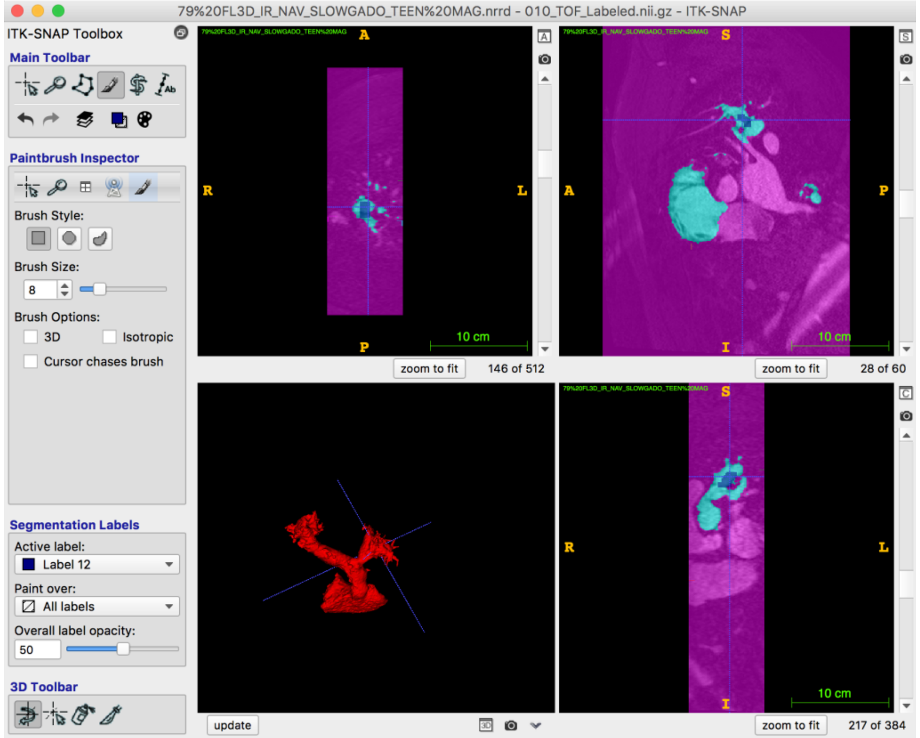

Labeling the left pulmonary artery in ITK SNAP (dark blue)

Methods: Multi-Atlas Segmentation

- Cardiac MRIs are often difficult to register between people due to the variability of anatomy
  - Anatomical landmarks placed to solve this issue
- **After landmarking a homography matrix was used to map points from atlas image to corresponding points from unknown image**
- Next step was deformable registration to further align images
- Followed by majority vote method to complete the segmentation
  - Determined for each voxel in each atlas whether or not the voxel is RVOT
  - If most say it is RVOT, it is labeled as such in the final segmentation

Methods: Multi-Atlas Segmentation

- Cardiac MRIs are often difficult to register between people due to the variability of anatomy
  - Anatomical landmarks placed to solve this issue
- After landmarking a homography matrix was used to map points from atlas image to corresponding points from unknown image
- **Next step was deformable registration to further align images**
- Followed by majority vote method to complete the segmentation
  - Determined for each voxel in each atlas whether or not the voxel is RVOT
  - If most say it is RVOT, it is labeled as such in the final segmentation

Methods: Multi-Atlas Segmentation

- Cardiac MRIs are often difficult to register between people due to the variability of anatomy
    - Anatomical landmarks placed to solve this issue
- After landmarking a homography matrix was used to map points from atlas image to corresponding points from unknown image
- Next step was deformable registration to further align images
- **Followed by majority vote method to complete the segmentation**
    - **Determined for each voxel in each atlas whether or not the voxel is RVOT**
    - **If most say it is RVOT, it is labeled as such in the final segmentation**

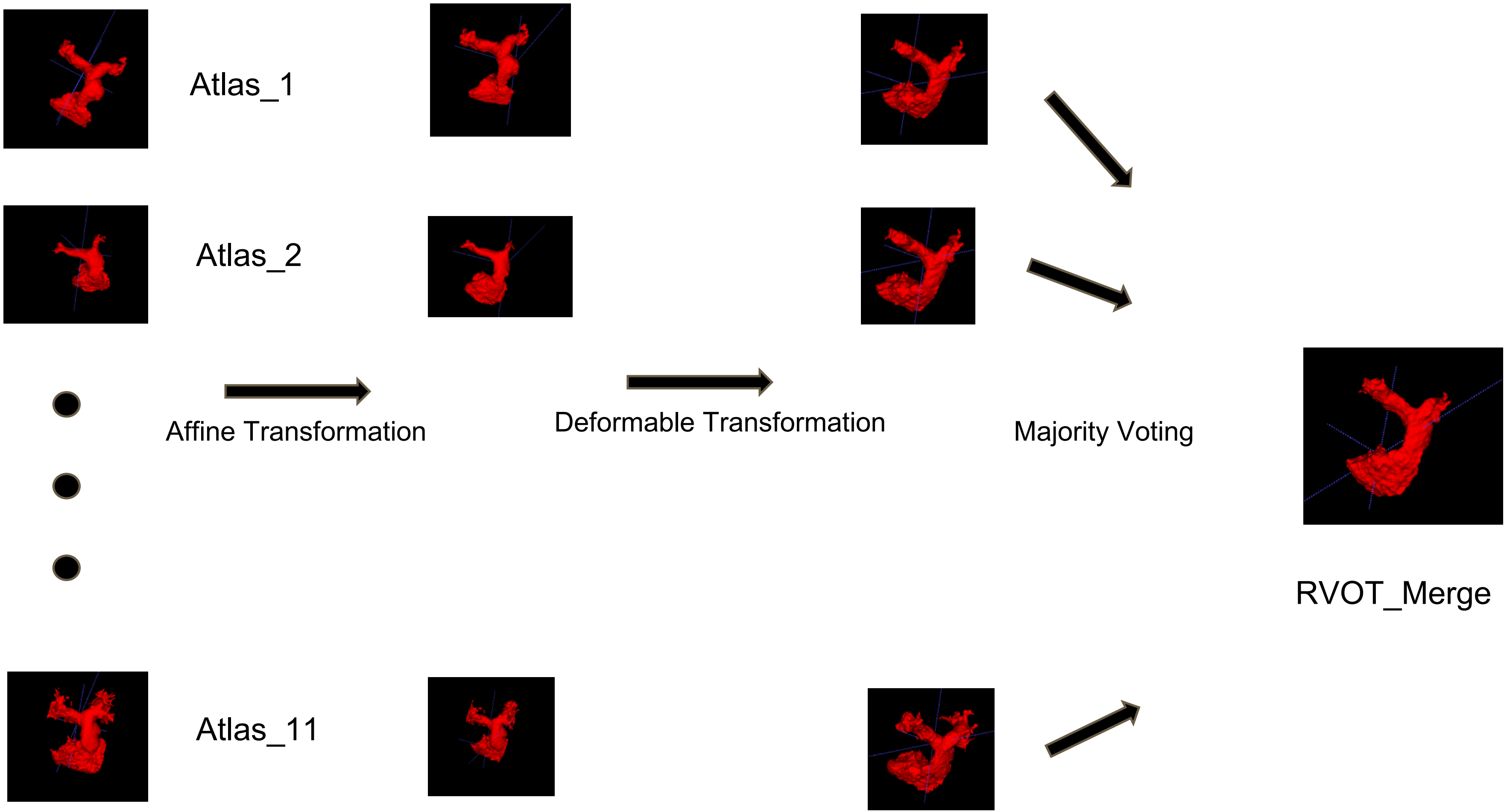

Atlas_1
Atlas_2
Atlas_11
Affine Transformation
Deformable Transformation
Majority Voting
RVOT_Merge

Methods: Validation Steps

- Calculate the Dice Overlap Score between "RVOT_Merge" and the ground truth segmentation
- Use c3d verbose -overlap command line tool to calculate the overlap region
- Visualize the overlap region on Paraview software

Results

Table 1: Overlap Metrics Between Ground Truth Segmentation and 11-Atlas Label Fusion Segmentation Result

For 5 iterations of greedy registration during deformable transformation step

Target Image	Matching voxels in result	Matching voxels in master segmentation	Size of overlap region	Dice similarity coefficient	Jaccard coefficient (intersection / ratio)
1	113320	69857	53850	0.587956	0.416386
2	282040	354430	205877	0.646934	0.478124
5	79005	110019	64980	0.687532	0.523846
6	833699	108751	70217	0.73097	0.576007
7	76598	199570	70490	0.510486	0.34272
8	233737	444087	179449	0.529486	0.360068
18	97481	117814	80338	0.746306	0.595286
22	325236	633749	293279	0.611645	0.440553
25	276569	194370	158876	0.67472	0.509115
27	63520	123761	49692	0.530668	0.361163
30	539569	116154	104040	0.317329	0.188587

Mean of dice scores: .5976	**Standard deviation of dice scores:** .1232

Dice Overlap Between Ground Truth Segmentation and Multi-Atlas Segmentation Result

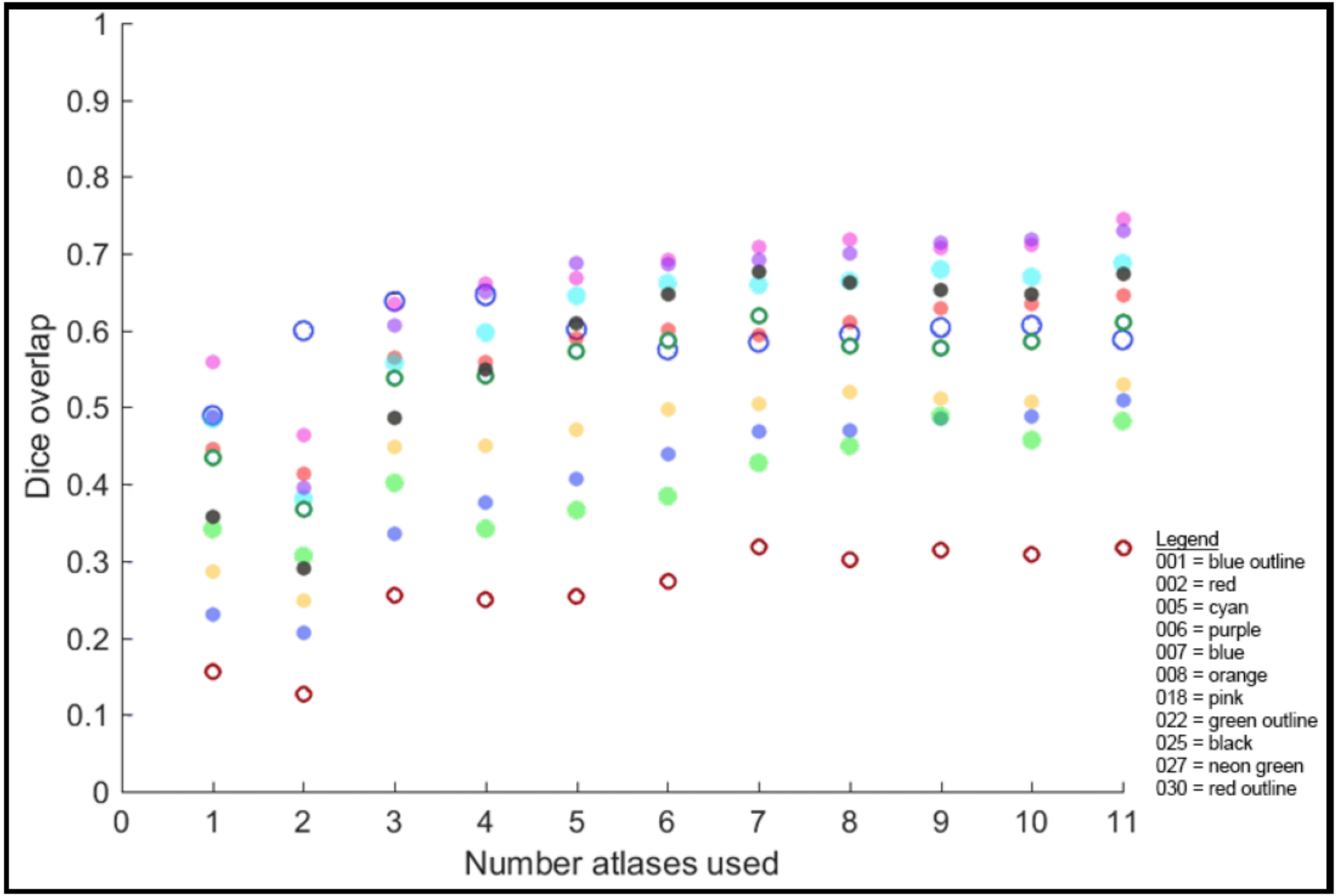

Figure 5: *Overlap metric for number of atlases used to produce each result, 5 iterations of greedy registration*

Mesh Overlaps between Ground Truth and 11-Atlas Results For Selected Images

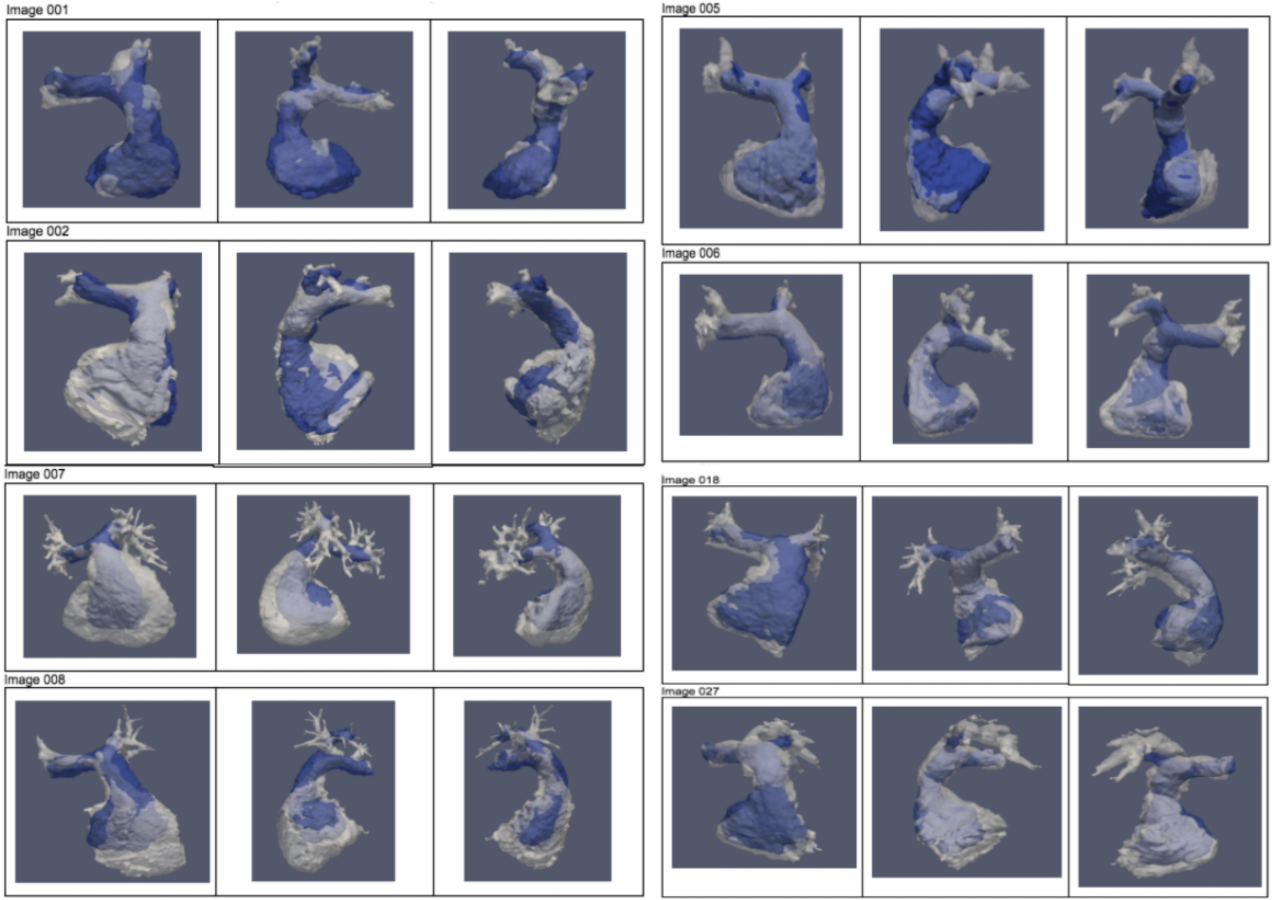

***Figure 6**: For selected images 1, 2, 5, 6, 7, 8, 18 and 27. The white mesh is the master segmentation, and the blue mesh is our results from performing multi-atlas segmentation on each target image from 11 atlases, using 5 iterations of greedy registration in the deformable transformation step.*

Dice Overlap Plots Between Ground Truth Segmentation and Multi-Atlas Segmentation Result For Image 018, Increasing Iterations of Greedy Registration during Deformable Registration

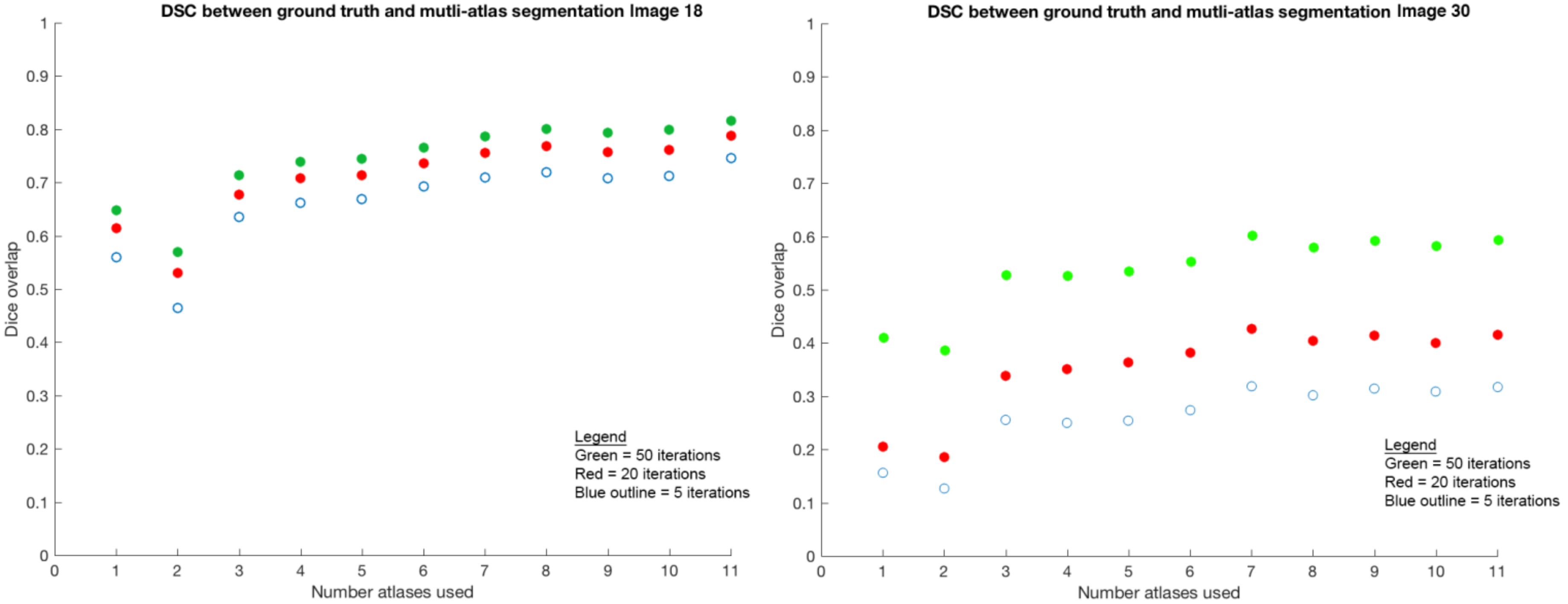

Figure 7: *Dice overlap metric improves with increased iterations of greedy registration during deformable registration across all multi-atlas segmentations of image 18*

Results

Table 2: Image 018 Overlap Metrics Between Ground Truth Segmentation and 11-Atlas Segmentation Result Increasing Iterations of Greedy Registration during Deformable Registration

# Iterations	Matching voxels in result	Matching voxels in master segmentation	Size of overlap region	Dice similarity coefficient	Jaccard coefficient (intersection / ratio)
5	97481	117814	80338	0.746306	0.595286
20	105973	117814	88190	0.78816	0.650383
50	114177	117814	94711	0.816506	0.689911

Overlap metric improves with increased iterations of greedy registration during deformable registration between 11-Atlas segmentation result and ground truth.

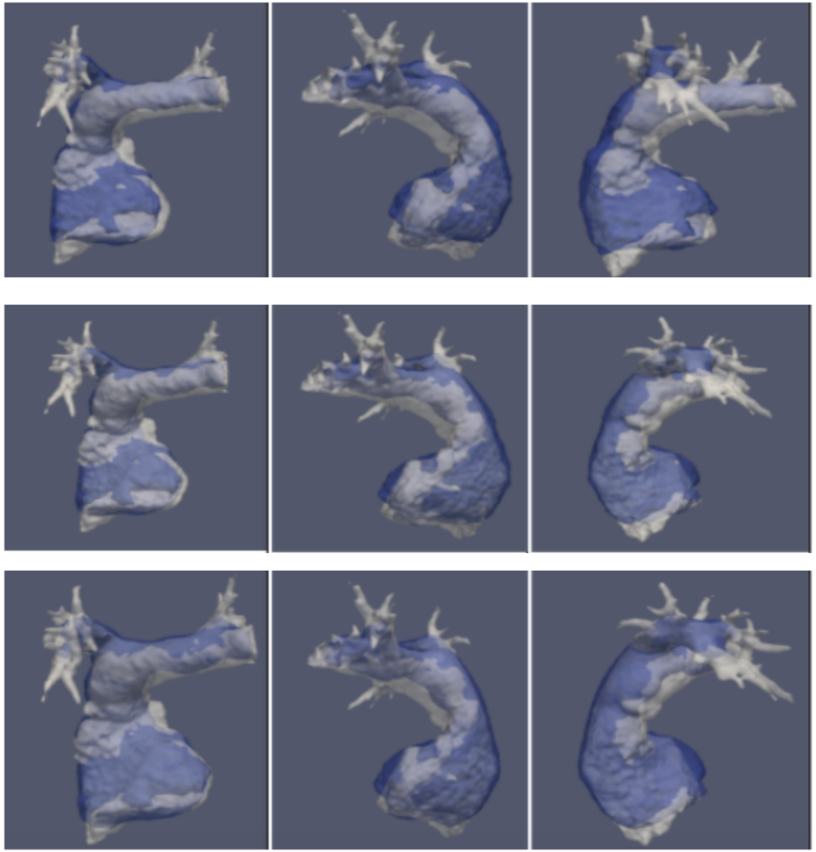

Figure 8: *Image 18 segmentation using 11 atlases at 5, 20, 50 iterations of greedy registration top to bottom*

Conclusions and Future Works

- Created a tool to automatically segment the RVOT in MRI data for ToF patients
  - Not as accurate as anticipated
- Future work
  - Increase consistency of manual segmentation and landmark placement
  - Further optimization of deformable registration to improve accuracy of individual candidate segmentations
  - Combine multi-atlas segmentation method with other strategies (Learned bias correction, CNNs, etc.)